

# A Lattice Model For the Kinetics of Rupture of Fluid Bilayer Membranes

Luc Fournier and Béla Joós\*  
*Ottawa Carleton Institute of Physics*  
*University of Ottawa Campus*  
*Ottawa, Ontario, Canada, K1N-6N5*

We have constructed a model for the kinetics of rupture of membranes under tension, applying physical principles relevant to lipid bilayers held together by hydrophobic interactions. The membrane is characterized by the bulk compressibility (for expansion)  $K$  and the thickness of the hydrophobic part of the bilayer thickness  $h$ . The model is a lattice model which incorporates strain relaxation, and considers the nucleation of pores at constant area, constant temperature, and constant particle number. The particle number is conserved by allowing multiple occupancy of the sites. An equilibrium "phase diagram" is constructed as a function of temperature and strain with the pores total surface and distribution as the order parameters. With parameters relevant to saturated phosphatidylcholine (PC) lipid membranes, well defined regions of "no pores", "protopores (non-critical pores)", "single hole rupture", and "multi-hole rupture" are found. The effect of edge healing (transformation from a hydrophobic to a hydrophilic edge) has been included. The boundaries between the different regions are very sharp. At room temperature, rupture is predicted at 3.75% strain, in accord with recent experiments on saturated chains. The model is also shown to be applicable to super-thick membranes. The strain at rupture is determined by the free energy of the lipid bilayer. We also present free energy curves as a function of total pore surface for various values of tension and temperature, and discuss the fractal dimension of the pore edge.

PACS numbers: 87.16.Dg, 87.16.Ac, 87.14.Cc, 68.60.Dv, 05.10.Ln

## I. INTRODUCTION

Fluid bilayer membranes separate the contents of cells from their surroundings. The stability of the fluid membranes under external perturbations is consequently of vital importance. In particular, if ruptured the functions of the cell will be disabled. Rupture or lysis can be achieved in a number ways: mechanically, by suction through a pipette, electrically by the electrocompressive forces that will act on the polar heads of the lipids [1, 2, 3, 4, 5, 6], and by osmotic swelling of the cell [7, 8, 9]. With the rapid progress in microscopic manipulation techniques, the number of experimental studies of the mechanical properties of the cell is rapidly increasing and we only quoted a few examples of recent work [10]. For the bilayers studied, there is a significant degree of consensus on the order of magnitude of the quantities involved. For phosphatidylcholine (PC) bilayers, area expansion seems to be only 2% to 4% before rupture. The corresponding external tension is of the order of  $10^{-3}$  to  $10^{-2}$  N/m [3, 11, 12, 13, 14]. It also seems that in liquid membranes rupture occurs via the nucleation of holes [15]. This is consistent with what is expected from structural considerations. Solid membranes as they go from brittle to ductile, experience rupture kinetics which evolve from processes dominated by crack formation to hole formation [16]. Pore sizes can range from nano- to micro-meter in radius. In electroporation experiments pores can last several microseconds [2, 3, 4, 5, 17]. Using mechanical means, namely micropipette extrusion on vesicles, pores can be kept open for several seconds before resealing [18, 19]. Pore formation can also serve a positive purpose in drug delivery and gene therapy [20, 21, 22].

Models of membrane rupture have been developed for a number of years. Most theories to date derive from a model suggested by Litster a quarter of a century ago [23]. It explains the stability in terms of a pore edge energy, or line tension. Under lateral stretching a membrane will by the creation of a pore reduce its surface energy. But as long as the total edge energy created by the pore exceeds the gain in surface tension, the membrane will be stable. The model defines a critical pore size and an energy barrier for the creation of an irreversibly growing pore. It has been extended and applied by other groups in particular to electric breakdown situations [2, 24, 25]. Shillcock and Boal also investigated the effect of temperature on membrane stability [26]. Temperature increases the entropy of the pore lowering its free energy. Even at zero tension, a minimum edge energy is required for stability. Netz and Schick developed a mean-field theory of the fluid bilayers as stacks of diblock copolymers [27].

---

\*Electronic address: bjoos@science.uottawa.ca

Our model considers pore creation as a thermally activated process [28]. There is an important entropic element to the nucleation process. The relevant physical quantities in the bilayer have their origin in the hydrophobicity of the lipid tails of the molecules as very clearly discussed by Wortis and Evans in a recent review article [29]. They are the area compressibility  $K$  which results from the increased exposure of the hydrophobic tails as the membrane is stretched, and the line energy  $\lambda$  is the result of the exposure of these tails to water along the edge of the pore. In the model, the bilayer is characterized by an energy per site, essentially one molecule in size. It incorporates stress relaxation as a pore is created and grows. Pore-pore interactions are automatically taken into account. An equilibrium phase diagram is constructed determining regions of no pores, non-critical pores (or protopores), single hole rupture and multiple hole rupture. The phase diagram is in terms of the temperature and the area expansion of the membrane. The critical temperatures scale with the strength of the hydrophobic interaction which to first order is linked to the length of the tails of the lipids. With parameters appropriate to pure phosphatidylcholine (PC) lipid bilayers, we find that rupture occurs at 3.75% at room temperature in accord with most recent experimental results with saturated chains [13, 14]. This predicted value applies to low strain rate since the membrane as it is remains in mechanical equilibrium. We also predict the possibility of a multiple hole rupture scenario for normal membranes, and for very thick membranes, a permissible area close to 50%. The following two sections develop the model. We first lay its physical foundations, and then present our Ising like model, which is solved using Monte Carlo simulations. We continue with the results and finish with a discussion of the possible extensions of the model.

## II. PORE CREATION

Upon area increase, stress will build up in the membrane. As mentioned earlier, being a liquid the most likely stress release mechanism will be the formation of holes or pores. Let us imagine that a hole has appeared through thermal induced stress fluctuations. The question will be whether the gain in energy occasioned by the relaxation of the surfactants will counterbalance the energy loss through exposure of the molecules to the solvent. If this is the case, the hole will continue to grow into a large pore that will permit the system to relax almost entirely. For now, we assume the process to be purely planar. Whether fluctuations in the third dimension are important is an open question. At first thought they do not seem predominant.

Assuming an elastic regime for small expansions on a lattice of relaxed size  $a_m$ , for stresses that are not too great, the energy associated with a stretching area of the membrane  $\Delta a = a_{total} - a_m$  is given by

$$E_m = \frac{1}{2} K a_m \left( \frac{\Delta a}{a_m} \right)^2, \quad (1)$$

But if a hole is inserted, some of this stress will be relieved. Nevertheless, the edge of the new pore will now be exposed to water. As the tails are hydrophobic, this will result in an increase of the energy proportional to the perimeter of the pore. For simplicity, we will assume the pore to be circular. In the presence of a pore, the energy of a stretched membrane then becomes

$$E_m(a_p) = 2\lambda\sqrt{\pi a_m} \left( \frac{a_p}{a_m} \right)^{1/2} + \frac{1}{2} K a_m \left( \frac{\Delta a - a_p}{a_m} \right)^2, \quad (2)$$

where  $a_p$  is the area of the pore. The parameters  $\lambda$  and  $K$  represent the line tension and the compressibility respectively. The first term in Eq. (2) is the total line energy, which represents the loss of energy on the perimeter of the circular hole. The second term, the surface energy, is the loss in energy resulting from the relaxation of the membrane induced by the hole, which augments the density of particles in the rest of the membrane. For lipids in general, typical line tensions  $\lambda$  are of the order of  $10^{-7}$  mN, so the edge energy of a 1nm radius pore is of the order of  $15\text{-}45 k_B T$  at room temperature [18]. For PC's with saturated chains, the compressibility  $K$  is approximately 230 mN/m [14].

For reasonably large systems, the energy barrier to rupture is given by  $\lambda^2 \pi / K (\Delta a / a_m)^{-1}$  and occurs for a pore area  $a_p = (\lambda a_m \sqrt{\pi} / K)^{2/3}$ . When  $a_p$  exceeds that critical value, the pore will grow till the membrane reaches the minimum energy configuration  $a_p = \Delta a$ . This argument predicts a barrier height of the order of  $10^3 k_B T_{room}$  for experimentally observed stretches, such as  $\Delta a / a_m = 4\%$  and a membrane of total area  $a_m = 1 \mu\text{m}^2$ , typical for PC membranes. It implies, as mentioned above, that the entropic component is very significant.

In an actual membrane, several small pores could be nucleated, as the energy of a pore of the size of a particle in a stretched membrane is of the order of  $k_B T_{room}$ . So for a given value of the expansion and temperature, there would be a distribution of pore sizes. Shillcock and Boal, as mentioned in the introduction, investigated one aspect

of temperature effects: the decrease in the free energy of the hole as its edges meander[26]. They considered a two-dimensional, self-avoiding, tethered manifold consisting of spherical beads (vertices) linked by flexible tethers (bonds). A hole was generated and its time evolution was studied by Monte Carlo simulation. Eq. (2) forms the basis of the zero temperature energetics. But at finite temperature, bonds can be broken or reformed, and the hole can change shape and size. Shillcock and Boal find that the minimum value of  $\lambda$ , even at zero tension is no longer zero but some finite value  $\lambda^* a = 1.24 k_B T_{room}$ , where  $a$  is the molecular size on the edge of the pore.

### III. THE MODEL

What we are trying to simulate is a thermally activated nucleation process, it is therefore natural to consider a model amenable to a Monte Carlo simulation. For ease of computation we consider a lattice model similar to the well-known Ising model for binary mixtures, and consider the equilibrium phase diagram of the system as a function of temperature and area expansion. This will reveal the expected scenarios of rupture as the membrane is expanded slowly, quasi-statically, so that the membrane remains in thermodynamic equilibrium at every step of the way. We will limit ourselves to two-dimensions, and to represent an isotropic liquid we will use a hexagonal lattice (6 closest neighbors). We begin by presenting the standard binary mixture model (SBMM) as applied to our problem and then describe the modifications that we have made to it to incorporate the stress relaxation that occurs when a hole is created. In the SBMM, every site can be in either of two states, in our case “ $a$ ” or “ $h$ ”, representing respectively sites occupied by a lipid or a hole. The site occupancy variable  $s_i$ , is equal to 1 if the site is in an “ $a$ ” site and 0 if it is in an “ $h$ ” site. The indices  $i$  and  $j$  run from 1 to  $N$ , where  $N$  is the total number of sites. Let  $J^{aa}(r_{ij})$ , or its compact form  $J_{ij}^{aa}$ , be the interaction between two lipids separated by a distance  $r_{ij} = |\mathbf{R}_i - \mathbf{R}_j|$ , where  $\mathbf{R}_i$  is the position vector of site  $i$ . In a similar way, we define  $J^{hh}(r_{ij})$  and  $J^{ah}(r_{ij})$ . The microscopic Hamiltonian  $H$  consists of the sum of all interactions:

$$H = \frac{1}{2} \sum_{ij} (J_{ij}^{aa} s_i s_j + J_{ij}^{hh} (1 - s_i)(1 - s_j) + J_{ij}^{ah} [s_i(1 - s_j) + s_j(1 - s_i)]). \quad (3)$$

Expanding Eq. (3), we have, regrouping terms in powers of  $s_i$ :

$$H = \frac{1}{2} \sum_{ij} (J_{ij}^{hh} + 2(J_{ij}^{ah} - J_{ij}^{hh}) s_i + (J_{ij}^{aa} + J_{ij}^{hh} - 2J_{ij}^{ah}) s_i s_j). \quad (4)$$

The total number of sites  $N$  is fixed. This model is usually studied in the canonical or grand canonical ensemble. In the canonical ensemble occupied ( $a$ ) and empty ( $h$ ) sites are interchanged to preserve the total number of particles. The conventional canonical model would be used if we were interested in the phase separation of a system, which is not our case. In the grand canonical ensemble, the only dynamics that would be observed is the distribution of the holes. Neither model is suitable to incorporate the relaxation created by the appearance of a hole. We start with the SBMM in the canonical ensemble with an initial total number of particles equal to the number of sites  $N$ . We now modify the model to impose the following constraints: the total area of the membrane stays constant as holes are created and the total number of lipids stays constant. These lead to the following changes in the dynamics. (i) Occupied sites, when holes are created, now contain more than one particle, actually  $N/(N - n_h)$ , where  $n_h$  is the number of hole sites at a given time. The occupancy variables  $s_i$  still only take the values 0 or 1, but the energy in the membrane has to be rescaled to take into account the increased occupancy of the occupied sites. As a hole site appears the density in the membrane increases. (ii) To avoid overestimating the line energy along a hole due to the increased occupancy of the sites along the edges of holes, a negative line energy correction  $\Delta E_{line}$  has to be added which is evaluated in Section III B below. (iii) Finally the nucleation of hole sites relaxes the membrane and reduces the interparticle distance. In other words the total number of occupied sites determines the average interparticle distance. With  $n_h$  hole sites the interparticle distances appearing in the  $J_{ij}^{kl}$ , in particular  $J_{ij}^{kl}$ , have to be rescaled to the new values:

$$\tilde{r}_{ij} = \left( \frac{N - n_h}{N} \right)^{1/2} r_{ij}, \quad (5)$$

where the  $r_{ij} = |\mathbf{R}_i - \mathbf{R}_j|$  are the initial intermolecular distances.

Putting these three factors together:

$$\tilde{H}(\tilde{r}) = \frac{N}{N - n_h} H(\tilde{r}) + \Delta E_{line}, \quad (6)$$

where  $n_h$  is the number of empty sites, called holes, present in the membrane at a given time and  $N$  is the total number of particles in the membrane, or the initial size of the discrete lattice.

Combining the general form in Eq. (4) with the transformations in Eqs. (5) and (6), we have (omitting  $\Delta E_{line}$  from the next three equations)

$$\tilde{H}(\tilde{r}) = \frac{N}{N - n_h} \cdot \frac{1}{2} \sum_{ij} (J_{ij}^{hh} + 2(J_{ij}^{ah} - J_{ij}^{hh}) s_i + (J_{ij}^{aa} + J_{ij}^{hh} - 2J_{ij}^{ah}) s_i s_j). \quad (7)$$

which can be rewritten as,

$$\tilde{H}(\tilde{r}) = \frac{1}{2} \frac{N}{N - n_h} \left[ N J_{ij}^{hh} + (N - n_h) (J_{ij}^{ah} - J_{ij}^{hh}) + \sum_{ij} (J_{ij}^{aa} + J_{ij}^{hh} - 2J_{ij}^{ah}) s_i s_j \right], \quad (8)$$

and finally expanded to,

$$\tilde{H}(\tilde{r}) = \frac{1}{2} \frac{N^2}{N - n_h} J_{ij}^{hh} + \frac{N}{2} (J_{ij}^{ah} - J_{ij}^{hh}) + \frac{1}{2} \frac{N}{N - n_h} \sum_{ij} (J_{ij}^{aa} + J_{ij}^{hh} - 2J_{ij}^{ah}) s_i s_j. \quad (9)$$

There is no interaction potential between holes: the effects of a hole are to break bonds, creating a line energy, and to relax the surface, reducing the surface energy. Because  $J^{hh}(r_{ij}) = 0$  and by regrouping the constant term in the effective interaction, this last equation reduces to the form (with  $\Delta E_{line}$  restored):

$$\tilde{H}(\tilde{r}) = \frac{1}{2} \frac{N}{N - n_h} \sum_{ij} J(\tilde{r}_{ij}) s_i s_j + \Delta E_{line}, \quad (10)$$

where  $J(\tilde{r})_{ij} \equiv J^{aa}(\tilde{r}_{ij}) - 2J^{ah}(\tilde{r}_{ij}) + J_0$ , noted  $\mathbf{J}_{ij}$  in the future, is the effective interaction.  $J_0$  is determined by the total energy  $U_0$  per particle in the membrane which is unstretched and has no pores ( $U_0 = \frac{1}{2} \sum_i J(r_{0i})$  in our model). An estimate of  $U_0$  is given in the following section.

### A. THE INTERMOLECULAR POTENTIAL

The main contribution to the intermolecular potential  $\mathbf{J}$  is the nearest neighbor hydrophobic interaction  $J^{aa}(r)$ , which is determined by the structure and the nature of the lipid chains. We will follow here the arguments of Wortis and Evans [29], but with the values of physical quantities updated, when required, with the results in Olbrich et al. [13] and Rawicz et al. [14]. Forcing water to sit against a hydrophobic surface will increase the free energy by roughly  $\sigma = 40 \text{ mN/m}$ . On the edge of a pore, the line energy therefore scales as

$$\lambda = \sigma h, \quad (11)$$

where  $h$  is the hydrophobic height (heads not included) of the bilayer. For most PCs, this thickness is between  $3 \text{ nm} < h < 4 \text{ nm}$ . We can deduce the energy of a molecule by multiplying the line tension by the perimeter of a site, and divide by 2 to avoid double counting. Assuming that amphiphiles are of cylindrical shape with a cross section of  $a_0 = 0.5 \text{ nm}^2$ , an estimate of the energy per particle in the unstretched membrane is  $U_0 = -16.5 \times 10^{-14} \text{ mJ} = -40 k_B T_{room}$  ( $k_B T_{room} = 4.14 \times 10^{-18} \text{ mJ}$ ).

As seen before, the creation of a hole affects not only the effective number of particles on a site but also the average distance between them. Therefore, the growth of a pore allows the stretched membrane to relax, leading to a decrease in the lattice parameter. The drop in energy is determined by the compressibility  $K$  of the membrane, whose origin is also hydrophobic.  $K$  can serve as the starting point for the construction of an interaction potential. Assuming a

linear regime for small expansions of the cross section area of a lipid  $a$ , the energy per molecule can be written as  $C(a - a_0)$ , where  $a_0$  is the relaxed or equilibrium area. The proportionality factor  $C$  is expected to be of the order of  $\sigma$ . For the repulsive force between polar heads, we chose a potential of the form  $D/a$ , where  $D$  is a positive constant. The minimum energy is set to  $U_0$ , the energy per molecule in an unstressed membrane. Combining these factors gives the energy per molecule

$$U(a) = C(a - a_0) + D(a^{-1} - a_0^{-1}) + U_0. \quad (12)$$

The requirement  $dU/da|_{a_0} = 0$  leads to the relationship  $D = Ca_0^2$ . Also, by comparing the curvature of this potential around the minimum with the surface energy of Eq. (2), we obtain  $C = \frac{1}{4}K$ . With an average compressibility of 230mN/m for most PCs with saturated chains [14],  $C$  is about 55mN/m, very close to  $\sigma$  as expected.

This energy per molecule is used to construct the shape of the main part of  $\mathbf{J}$ , the first neighbor hydrophobic interaction  $J^{aa}(r)$ . For practical reasons, this interaction is expressed as a function of the lattice parameter in the hexagonal grid:

$$J^{aa}(r) = 2\sqrt{3}K(r^2 - r_0^2) + \frac{8a_0^2}{\sqrt{3}}\left(\frac{1}{r^2} - \frac{1}{r_0^2}\right). \quad (13)$$

In such a lattice, the area  $a$  and the nearest neighbor distance  $r$  are related by  $a = \sqrt{3}r^2/2$ . The other term in  $\mathbf{J}$ ,  $J^{ah}(r)$ , is a correction that is a measure of the deformation and consequently the stress field created around a hole. Because the correlation in a liquid decays exponentially [30],  $J^{ah}(r)$  will be a weak repulsive exponential tail which, in our model, does not act on the first neighbors. We usually sum the interactions from the  $2^{nd}$  up to the  $5^{th}$  neighbors. Explicitly, this potential has the form,

$$J^{ah}(r) = Ge^{-r/r_0}, \quad (14)$$

where the amplitude parameter  $G$  is set arbitrarily to be about 10% of the main well. The amplitude of the exponential term will be shown to have little effect on the results.

This last interaction makes the shape of the potential slightly different from the one derived in Eq. (13). The value of  $J_0$ , has to be adjusted so that the total energy per molecule at equilibrium is equal to  $U_0 = \frac{1}{2} \sum_i J(r_{0i})$  in a perfect hexagonal lattice. Therefore, the artificially induced stress field shown in Eq. (14) does not affect the depth of the potential.

### B. The line energy correction

The surface of the membrane and the number of particles are both kept constant leading to the weight of an occupied site being slightly different from one. This renormalization is perfectly consistent with the surface energy of a pore which scales as  $NKr^2$ . But for the line energy, which is proportional only to the perimeter of a hole, there is a dimension problem. Because each site contains now more than one particle, the correction will be to count only the ones that are on the edge, not the deeper ones. In a hexagonal lattice, a particle facing a hole will normally lose two bonds, which corresponds to an interaction of  $\frac{1}{2}[6J^{aa}(\tilde{r}) - 4J^{aa}(\tilde{r})] = J^{aa}(\tilde{r})$ . This way, the line energy per particle on the edge of a pore per unit length can be written as  $-J^{aa}(\tilde{r})/\tilde{r}$ , which is a positive value given that  $J^{aa}(r) < 0$ . With this in mind, we can write the correct expression for the line energy as

$$E_{line} = \frac{-J^{aa}(\tilde{r})}{\tilde{r}} L^{ah} r \quad (15)$$

where  $L^{ah}$  is the number of particle-hole interactions (between the sites), and therefore the number of sites along the perimeter of all the pores in the membrane. This way,  $L^{ah}r$  represents the perimeter of the entire interface particles-holes. Due to the renormalization factors given by Eqs. (6) and (5), the equivalent expression in the model for the line energy is given by

$$E_{line}^{model} = \left(\frac{N}{N - n_h}\right) \frac{-J^{aa}(\tilde{r})}{\tilde{r}} L^{ah} \tilde{r}. \quad (16)$$

The negative correction required by the program is then

$$\Delta E_{line} = E_{line} - E_{line}^{\text{model}} = -J^{aa}(\tilde{r})L^{ah} \left( \frac{r}{\tilde{r}} - \frac{N}{N - n_h} \right), \quad (17)$$

which can be simplified to

$$\Delta E_{line} = \frac{1}{2} J^{aa}(\tilde{r}) L^{ah} \frac{n_h}{N - n_h} \quad (18)$$

if we recall the correction factor of Eq. (5) and assume that  $n_h \ll N$ . This small correction is only applied to  $J^{aa}$ , as the corrections of the tail were neglected.

### C. The healing on the edge of a pore

Another effect that we consider is the rearrangement of the molecules on the edge of a pore to reduce the hydrophobicity. The amphiphiles on the edge can arrange themselves in an arc shape to produce a bevelled edge. We call this healing of a the edge of the pore. Modeling this is quite complicated because pores keep evolving, shrinking or growing. To simplify the problem, we will only consider one possible bending angle (90 deg) and 6 possible horizontal orientations, which correspond to the 6 neighbor sites. As shown in figure 1a, one bended site on the edge of a pore will then represent the entire arc. A bended site will now interact differently with its 6 neighbors. Holes in front of a bended site will lower the energy, as a site being oriented through another particle will not be favorable because of the heads repulsion. However, a site facing away from a hole will definitely be unfavorable, and so is the case for a site facing away from a particle. This last interaction will not be favorable because the gap created between the particles can act as a channel for water. Finally, two cases are considered impossible: an amphiphile directly facing away from a hole and an amphiphile directly facing another one. As those energies are small compared to the real intermolecular interactions, we will define for simplicity all the favorable interactions as  $\alpha$  (a negative value) and the unfavorable ones as  $\beta$  (positive). All the possible interactions are summarized in figure 1b.

The energy  $S$  associated with a bended site is then reduced to three degenerate cases (assuming that we eliminate the impossible cases discussed earlier):

$$S = \begin{cases} 1\alpha + 5\beta; & \text{when } n_{h,front} = 1 \\ 2\alpha + 4\beta; & \text{when } n_{h,front} = 2 \\ 3\alpha + 3\beta; & \text{when } n_{h,front} = 3 \end{cases}, \quad (19)$$

where  $n_{h,front}$  is the number of holes facing the bended site. This energy can be rewritten as

$$S = (\alpha - \beta)n_{h,front} + 6\beta. \quad (20)$$

The energy difference between a hydrophobic and a beveled edge is small [29]. A reasonable choice is to choose  $\alpha = -0.25 U_0$  and  $\beta = 0.1 U_0$  to have a healing energy of  $0.10 U_0$  along a straight edge.

This energy is completely separated from  $H$  and all the corrections associated with it. We are therefore in the approximation that even if the occupancy of the sites is greater than one, only one particle on each site can be healed. However, the metropolis algorithm will again be used to create and annihilate orientations. The only time that these healing effects will interfere with the main system is when a site containing a bended particle becomes a hole and when a hole fronting a healed particle is revived. Those situations correspond respectively to a healed pore that is either growing or shrinking. Removing the healed edge every time that the shape of a pore is modified would consist in an error in the dynamics. To correct this situation, swap functions have been included in the model to be able to move the edge of a pore as it is evolving in time. More precisely, if a pore is growing by converting a healed site onto a hole, the swap functions will translate this oriented particle backward, therefore on the new edge. Moreover, if it is shrinking, it will be possible to forward the oriented particle onto the edge of the smaller pore.

Because this energy is of the order of  $k_B T_{room}$ , the healing effects in this model will be almost totally entropic at room temperature. In other words, except for low temperatures, the edge of a stable pore is only about 50% healed. Nevertheless, it does increase hysteresis effects in the creation and closing of pores, as physically expected.

## D. Programming and Analysis

To create and recover holes in the membrane up to an equilibrium point, we use the Metropolis algorithm in the Monte Carlo simulation. The mass of a hole is zero, but the mass of the system or number of particles is conserved through the renormalization of Eq. (6). Although the occupation of sites changes as the simulation evolves, detailed balance is satisfied because each configuration of pores has a uniquely defined energy. This energy does not depend upon the path followed to reach it. The transition probability between a given initial and final configuration will also be unique and reversible. If we choose an occupied site with the same probability than an empty site, that is, we select particles or holes according to their surface distribution, the acceptance rule will be given by

$$acc(i \rightarrow f) = \min(1, \exp \left[ - \left( \tilde{H}_f - \tilde{H}_i \right) / k_B T \right] ), \quad (21)$$

in order to respect detailed balance. This acceptance rule is the usual one for a Monte Carlo simulation in the canonical ensemble. Finally, periodic boundary conditions are considered.

The approach is highly efficient and large systems can be studied, up to  $10^7$  particles. Usually within a 100 samplings per site, the equilibrium state is reached.

## IV. RESULTS

We study the scenario of rupture through an “equilibrium” phase diagram that looks at the different qualitative changes in the distribution of pores as a function of stretching for temperatures around  $k_B T_{room}$ . This corresponds to slow (quasistatic) stretching rates that keep the membrane in a state of equilibrium with respect to the applied stress. In the case of a higher rate of expansion, larger stretches and therefore tensions will be needed to break the membrane [28]. Because we are considering thermally activated processes, higher temperatures in this model are equivalent to weaker interactions. The reduced temperature used is  $k_B T/U_0$ , where  $U_0$  is the energy of a particle in a relaxed lattice. To study the reversibility of membrane lysis, hysteresis curves were constructed to compare the number of holes and their distribution as we first stretch the membrane to rupture, and then let it relax to zero tension. This study revealed that the rupture transition is first order, with a strong hysteresis. The fractal dimensions of stable pores were computed at different temperature as a measure of their entropy and shape.

Bilayer membranes can form vesicles of a variety of shapes [29]. They are normally present in nature as spherical vesicles of radii between 1-10  $\mu\text{m}$  [13, 14, 29]. Our phase diagrams are for systems of area around  $5\mu\text{m}^2$ , corresponding to  $\sim 10^6$  particles. It is an interesting issue to see the dependence of rupture on the system size, if any. For systems larger than  $10^5$  particles, the rupture point stabilizes at a stretch of 3.75% at room temperature (Fig. 2). For smaller systems, we observe a significant increase. This increase, of course, is mainly due to the loss of entropy, but the energy barrier of Eq. (2) can also be shown to rise for smaller systems. Therefore, for all the simulations, except when specified, a lattice of 1.1 million phosphatidylcholine (PC) type amphiphiles is used.

### A. Phase diagram

Qualitatively, we can separate the membrane behavior in four regimes: the *no pore* region, where  $n_h < 1\%\Delta a/a$ , that is less than 1% of the new surface was converted into holes to relax the system; *protopores*, where the number of holes is between  $1\%\Delta a/a < n_h < 90\%\Delta a/a$  and the pores (group of holes) are of sizes not bigger than 2-3 particles; *rupture*, where the number of holes  $n_h > 90\%\Delta a/a$  are distributed in only a few massive pores ( $< 10$ ); and finally, *multiple rupture*, for  $n_h > 90\%\Delta a/a$  and the number of pores greater than 10. The transient case, where  $n_h < 90\%\Delta a/a$  with only a few pores on average, has never been observed at equilibrium.

In the full potential scheme for PCs (fig. 3a), at room temperature, we observe a first order transition between the *no pore* and the *rupture* regime at a stretch of  $\Delta a/a = 3.75\%$ . This seems to be in accordance with experimental results [13,14], which give a critical tension to rupture of  $\tau^* = 9 \pm 1$  mN/m with a compressibility of  $K = 240 \pm 10$  mN/m, giving a stretch of exactly  $\Delta a/a = 3.75\% \pm 0.20\%$ . Also, the membrane becomes unstable with no applied tension at  $k_B T/U_0 = 0.65$ , which is comparable to the value of 0.6 of Shillcock and Boal [26].

If we include only the main interaction  $J^{AA}(r_{ij})$ , we observe a slight increase in the rupture tension at higher temperatures, and also a reduction in the size of the protopore regime. The reason is that with no stress field, holes tend to coalesce. This directly reduces the protopore regime part of the rupture activation kinetics at higher temperatures. As protopores, or small non-stable pores have experimentally been observed [4], we are to believe that the exponential tail plays an important role in the kinetics of membrane rupture.

For both figures 3a and 3b, the bilayer lipid chain length was fixed at  $h^* = 3.5\text{nm}$ . To explore the applicability of the model, thicker membranes were considered: (i) with double length lipid chains,  $h^* = 7.0\text{nm}$  (Fig. 3c) and (ii) a super-membrane with  $h^* = 20.0\text{nm}$  (Fig. 3d). For the double membrane, the hydrophobicity  $\sigma$ , therefore the compressibility  $K$ , are the same as for the normal membrane. Only the line energy, and hence  $U_0$ , are doubled. The scale for the reduced temperature  $k_B T/U_0$  is therefore multiplied by a factor  $1/2$ . For the super-membrane with  $h^* = 20.0\text{nm}$ , the compressibility has been observed to be  $K = 100\text{mN/m}$  [31], which is smaller than the  $230\text{mN/m}$  for the PC membranes. We assumed for simplicity that the lateral size of the molecules remains unchanged. A line energy  $20/3.5$  times larger was therefore used, and  $U_0$  is increased by a total factor of 2.9. With those parameters, our critical stretch at room temperature is 41%, a little lower than the 50% observed experimentally [31, 32]. In addition to uncertainties in the basic parameters, another possible reason is that our potential defined in Eq. (13) assumes small stretches about a minimum, and therefore not stretches of 50%.

## B. Hysteresis

To illustrate the properties of the real dynamics, we show a single sample put through a full cycle of expansion and compression. This is done again in a quasi-static process, i.e., at each step the system is allowed to relax. As shown in Fig. 4, at low temperature, hysteresis effects are very strong. Rupture and healing occur through one pore. At high temperature, hysteresis is reduced and there are many more pores.

The healing effect on the edge of a pore plays a role in hysteresis. Once a stable hole is created, it is very likely that particles on its edge will heal. Closing the pore completely through the hysteresis loop will force some bended sites to face one another. As discussed previously, this is an impossible configuration. As a consequence, small holes will persist until smaller tension than expected.

## C. Shape of the pores

The shape of a pore is estimated from the scaling relationship between the pore area and its perimeter. At different temperatures for a stretching of 3% (just before rupture), we break the membrane by inserting a hole at the origin. After the pore is fully opened and stable, we compute the fractal dimension of this pore to get the proportionality between the area of a pore and its circumference. The results are plotted in Figure 5. The fractal dimension decreases as the temperature is raised. This is caused by increased irregularities along the edge of the pore.

At the temperature  $k_B T/U_0 = 0.65$  where rupture occurs spontaneously at zero tension, one would expect the scaling relationship applicable to a self-avoiding ring [26]. Or the area of the pore should scale as  $A = A_0 l^{3/2}$ , where  $l$  is the perimeter, and  $A_0$  a proportionality factor, not relevant here. In this case, our model gives a scaling relationship of  $A = A_0 l^{1.57 \pm 0.15}$  in agreement with this argument.

## D. Free energy

The plot of the free energy  $F$  of the system as a function of the number of holes cannot be obtained directly from the simulation, since the system will always stabilize around the number of holes that minimizes the free energy. One way to obtain this curve is by the technique known as umbrella sampling. It consists in adding to the initial Hamiltonian  $H$  a harmonic potential  $W(n_h)$ , known as a bias potential, centered at an arbitrary  $n_h^*$ . We let the system evolve to get occupation probabilities  $P_{bias}$  around a given  $n_h^*$ . This is repeated for a sequence of  $n_h^*$  spanning the range of  $n_h$ 's of interest. From the set of segments of  $P_{bias}$ , probabilities  $P'(n_h)$  for the unbiased system are obtained. These are linked together to generate the correct probability function  $P(n_h)$ . The free energy  $F$  is obtained directly from  $F = -\log(P) + C$ .

The big difference between the free energy curves plotted in Fig. 6 and the one predicted by Eq. (2) is the effect of entropy near  $n_h = 0$ . As discussed previously, without entropy, the barrier to rupture is physically prohibitive. Entropy can also shift the local minimum near zero pore size to a nonzero value, noted as the protopore regime. There is another shift near the global minimum, where the amphiphiles do not relax entirely when membrane rupture occurs. There is still a bit of tension. This effect, predicted by the theoretical model, is not entropic, but purely energetic, a contribution of the line energy to the final equilibrium state.



## V. CONCLUSION

We have developed a model for the rupture of a membrane held together by hydrophobic forces. In spite of their complex molecular structure lipid bilayer membranes offer an ideal model system as hydrophobicity is responsible for both the line energy and the bulk compressibility (for extension). Our minimal model explains current results on PC and thicker artificial bilayers for the tension and area expansion at rupture. The stability results of Shillcock and Boal [26] for unstressed membranes have also been reproduced. The model is robust in the sense that the essential features of the results are unchanged even if healing on the edge of the pore and the stress field around a pore are neglected. The model requires little computer time allowing the handling of real size vesicles. Entropic and nucleation effects are included naturally.

The structural integrity of a lipid bilayer is considerably affected by its composition; Biological membrane structure can be fairly complex. Different types of lipids, cholesterol, peptides, and proteins will play an important role in determining membrane stability. The model has the potential of handling these inclusions.

## Acknowledgements

The authors wish to thank Michael Wortis, James Polson, David Boal, Dennis Discher, and Martin Zuckermann for many stimulating discussions. The work has been funded by the Natural Sciences and Engineering Research Council (Canada).

- 
- [1] W. Harbich and W. Helfrich, *Z. Naturforsch.* **34A**, 1063-1065 (1979).
  - [2] I.G. Abidor, V.B. Arakelyan, L.V. Chernomodik, Y.A. Chizmadzhev, V.F. Patushenko, and M.R. Tarasevich, *Bioelectrochem. Bioenerg.* **6**, 37-52 (1979).
  - [3] D. Needham, and R.M. Hochmuth, *Biophys. J.* **55**, 1001-1009 (1989).
  - [4] C. Wilhelm, M. Winterhalter, U. Zimmermann, and R. Benz, *Biophys. J.* **64**, 121-128 (1993).
  - [5] M. Winterhalter, *Colloids and Surfaces A* **149**, 161-169 (1999).
  - [6] S.Y. Ho and G.S. Mittal, *Crit. Rev. Biotech.* **16**, 349-362 (1996).
  - [7] A. Ertel, A.G. Marangoni, J. Marsh, F.R. Hallett, and J.M. Wood, *Biophys. J.*, **64**, 426-434 (1993).
  - [8] B.L.-S. Mui, P.R. Cullis, E.A. Evans, T.D. Madden, *Biophys. J.*, **64**, 443-453 (1993).
  - [9] C. Taupin, M. Dvolaitzky, and C. Sauterey, *Biochemistry* **14**, 4771-4775 (1975).
  - [10] D. Boal, *Mechanics of the Cell* (Cambridge Univ. Press, Cambridge, 2001).
  - [11] J. Wolfe, M.F. Dowgert, and P.L. Steponkus, *J. Membrane Biol.* **86**, 127 (1985).
  - [12] E.A. Evans and D. Needham, *J. Phys. Chem.*, **91**, 4219 (1987).
  - [13] K. Olbrich, W. Rawicz, D. Needham, and E. Evans, *Biophys. J.* **79**, 321 (2000).
  - [14] W. Rawicz, K.C. Olbrich, T. McIntosh, D. Needham, and E. Evans, *Biophys. J.* **79**, 328 (2000).
  - [15] D.S. Dimitrov and R.K. Jain, *Biochim. Biophys. Acta.* **779**, 437 (1984).
  - [16] Z. Zhou and B. Joós, *Phys. Rev. B.* **56**, 2997 (1997).
  - [17] J. Akinlaja and F. Sachs, *Biophys. J.* **75**, 247 (1998).
  - [18] D.V. Zhelev and D. Needham, *Biochim. Biophys. Acta.* **1147**, 89 (1993).
  - [19] O. Sandre, L. Moreaux, and F. Brochard-Wyart, *Proc. Nat. Acad. Sci. (U.S.A.)* **96**, 10591 (1996).
  - [20] J.S. Remy, A. Kichler, V. Mordvinov, F. Schuber, and J.P. Behr, *Proc. Nat. Acad. Sci. (U.S.A.)* **92**, 1744 (1995).
  - [21] F.D. Ledley, *Hum. Gene Ther.* **6**, 1129 (1995).
  - [22] N.M. Correa and Z.A. Schelly, *Langmuir* **14**, 5802 (1998).
  - [23] J.D. Litster, *Phys. Lett. A* **53**, 193 (1975).
  - [24] A. Barnett and J.C. Weaver, *Bioelectrochem. Bioenerg.* **25**, 163 (1991).
  - [25] S.A. Freeman, M.A. Wang, and J.C. Weaver, *Biophys. J.* **67**, 42 (1994).
  - [26] J.C. Shillcock and D. H. Boal, *Biophys. J.* **71**, 317 (1996).
  - [27] R.R. Netz and M. Schick, *Phys. Rev. E* **53**, 3875 (1996).
  - [28] E. Evans and F. Ludwig, *J. Physics: Condens. Matter.* **12**, 315 (2000).
  - [29] M. Wortis and E. Evans, *Physics in Canada* **53**, 281 (1997).
  - [30] J.M. Ziman, *Models of Disorder* (Cambridge University Press, Cambridge, 1979) Chap. 3.
  - [31] D. Discher, Personal communication (2001).
  - [32] B.M. Discher, Y.-Y. Won, D.S. Ege, J.C.-M Lee, F.S. Bates, D.E. Discher, D.A. Hammer, *Science* **284**, 1143 (1999).

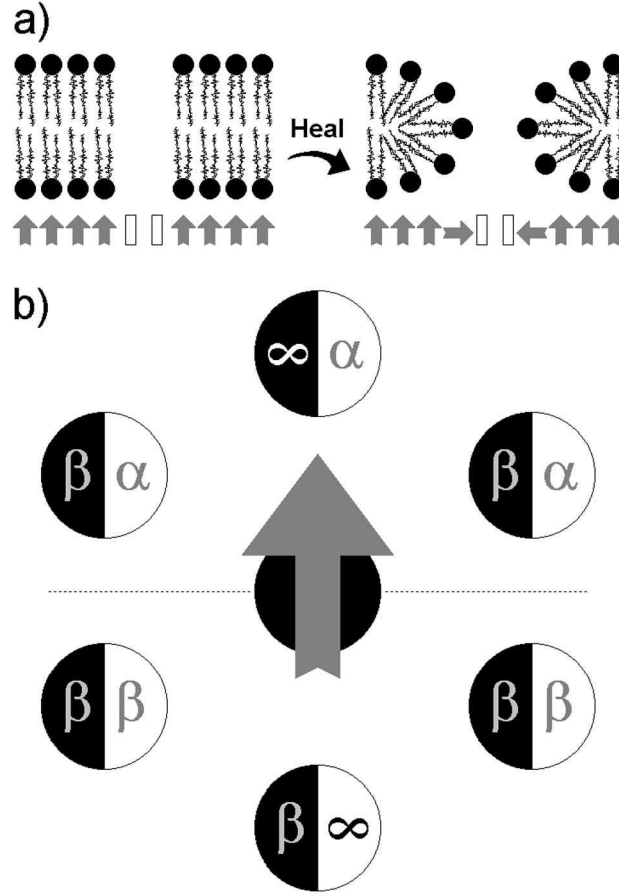


FIG. 1: (a) A hydrophobic edge changing to a beveled (or healed) edge with the spin representation of the model and (b), the possible interactions of an oriented particle with its 6 neighbors. Each of those sites can either be a particle (containing particle oriented or not) or a hole. We eliminate the two impossible interactions by setting their energies to infinity. All the other interactions are set to  $\beta$ , except for the three possible orientations facing holes that will have interaction energies of  $\alpha$ .

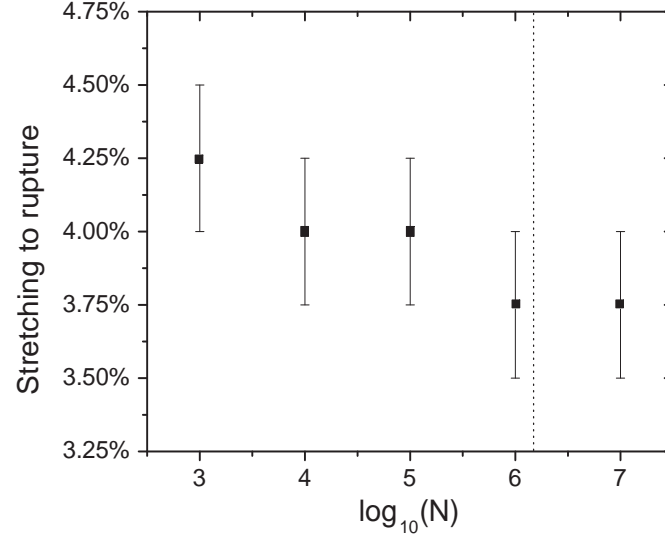


FIG. 2: Rupture point for different system sizes  $N$ , at room temperature for the PC model. Smaller systems are harder to break, as the probability of nucleating pores is lower. The dashed line represents the size of the system used for normal simulations, which corresponds to a vesicle of radius  $\sim 1\mu\text{m}$ .

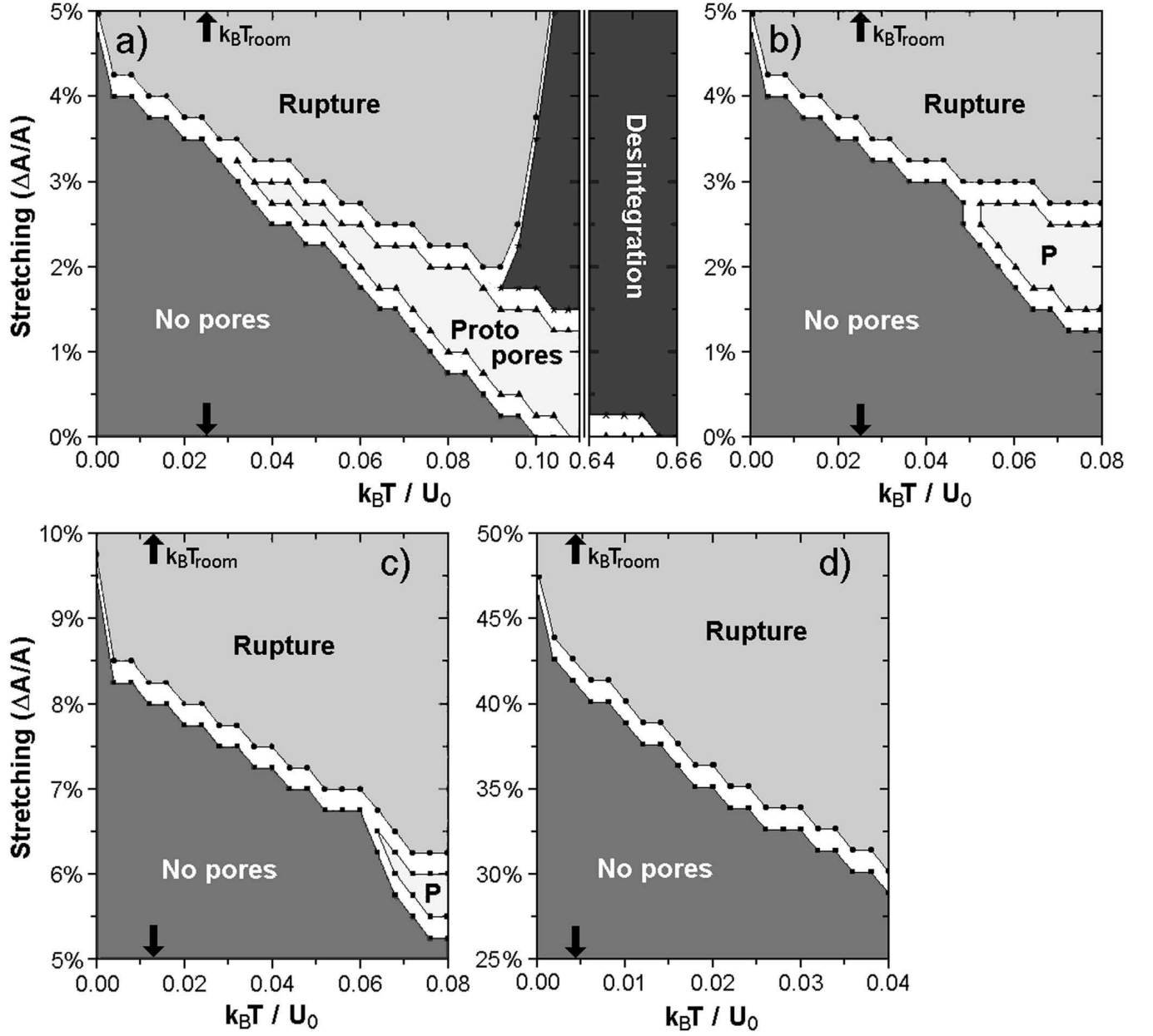


FIG. 3: (a) Phase diagram showing the distribution of holes with (a) the complete potential and (b) with only the hydrophobic interaction. If the stress field is not included, the rupture is much more abrupt and a higher stretching is needed to reach this point. (c) Results for lipids with chains double the length than those for PC chains ( $h^* = 7\text{nm}$ ), and (d) for a super-membrane with  $h^* = 20\text{nm}$ .

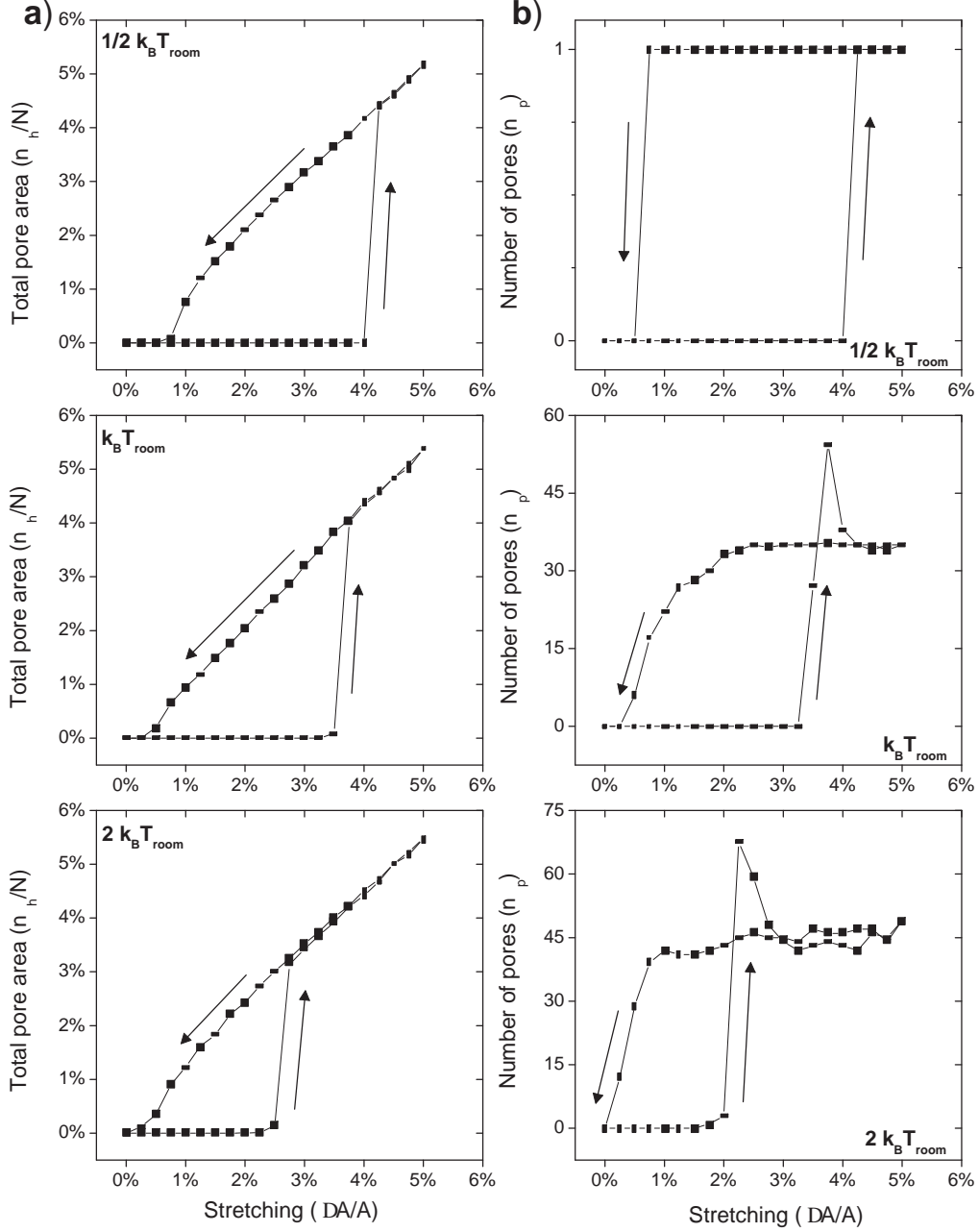


FIG. 4: Hysteresis curves: (a) total pore area and (b) number of pores for temperatures below, at, and above room temperature. For low temperatures, the rupture is abrupt and occurs around one hole with a very strong hysteresis. In the other limit, less hysteresis is present and everything changes gradually. At room temperature, both effects are observable with the intermediate protopore regime.

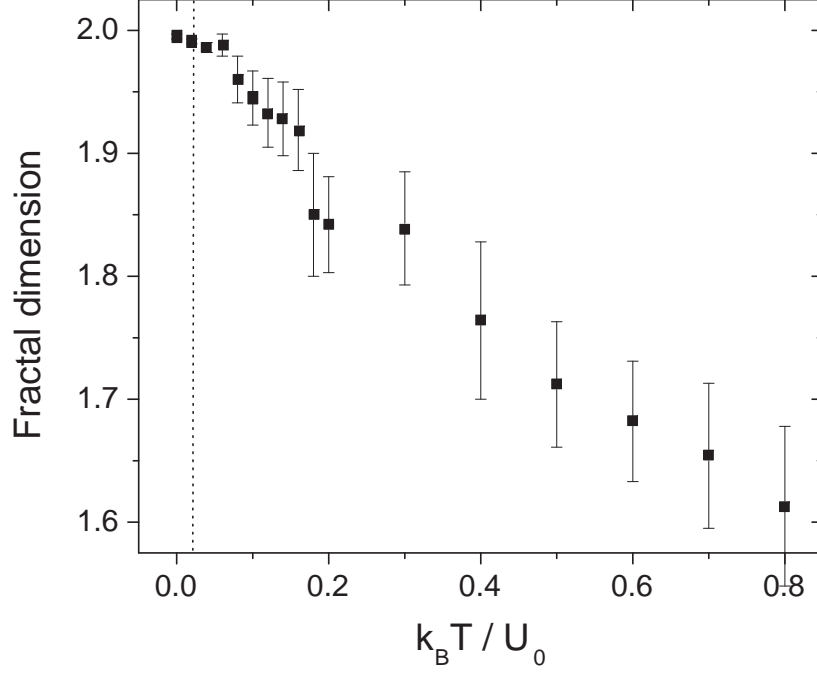


FIG. 5: The fractal dimension of a pore in a stretched membrane. This quantity is a measure of the regularity of the shape of the pore and its edge. As the temperature is increased, the hole becomes irregular and spreads over the whole membrane surface. The dash line indicates room temperature which corresponds to  $k_B T / U_0 = 0.025$ .

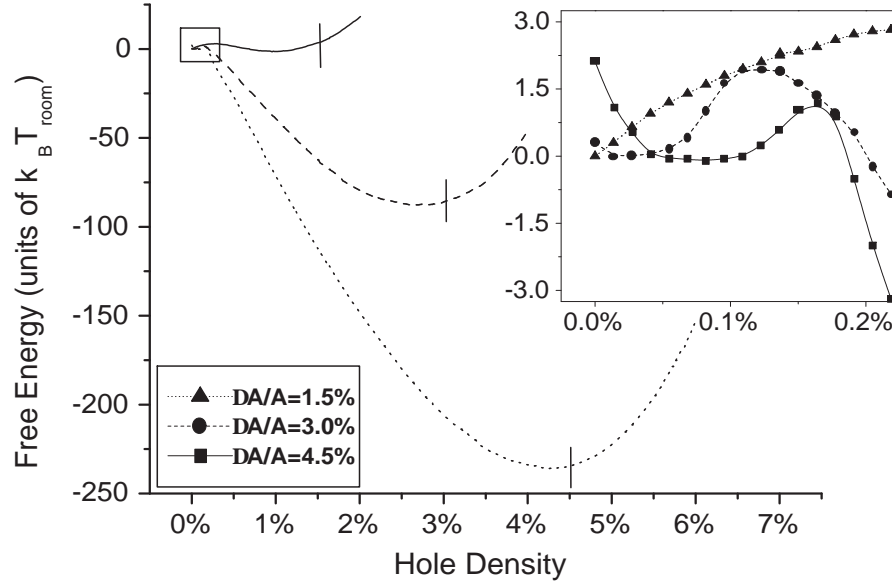


FIG. 6: Free energy curves as a function of the number of holes at room temperature, as given by the Umbrella Sampling method. For a weak extension, there is no protopore local minimum. For large tensions, a protopore regime appears with an average of 5–10 holes present in the membrane for  $N = 10981$ . At room temperature, we cannot observe this regime because the system settles in the global minimum.